Journal of the Korean Physical Society, Vol. 51, No. 6, December 2007, pp. 1897∼1900

Fabrication of Magnetic Nanowires by Using Laser Interference Lithography and Magnetic Analysis

J. H. Kang, S. G. Lee, H. M. Hwang and J. Lee*
Institute of Physics and Applied Physics, Yonsei University, Seoul 120-749

J. H. Song
Advanced Analysis Center, Korea Institute of Science and Technology, Seoul 130-650

(Received 19 June 2007, in final form 2 October 2007)

We have fabricated polycrystalline Fe nanowires by using laser interference lithography without any mask. The width of the wire is varied from 161 nm to 458 nm. The pitch is controlled by adjusting the angle between the two laser beams. All the magnetic wires clearly show in-plane uniaxial magnetic anisotropy, but the anisotropy is affected by the ratio of the width to the thickness.

PACS numbers: 42.82.Cr, 75.30.Gw, 61.46.+w
Keywords: Laser interference lithography, Magnetic nanowire, Magnetic anisotropy

I. INTRODUCTION

Recently, ferromagnetic nanowires have been attracting much attention because they are of practical importance in devices such as magnetic information transfer and logic devices [1–3]. This is possible because the magnetization direction is well-defined and stabilized in the direction of the wire axis due to the magnetic shape anisotropy [4, 5]. A large enhancement in the coercive field has been reported with decreasing wire diameter [6–8]. It is also reported that nanowires that are not circular in cross section show a shape anisotropy in the plane perpendicular to the wire axis [9].

The fabrication of an ordered array of magnetic nanowires can be carried out by using e-beam and X-ray lithography, in combination with evaporation techniques, in vacuum [10,11]. However, e-beam lithography is heavily time-consuming for large-area patterning. X-ray lithography requires synchrotron radiation facilities and masks that should be produced by using e-beam lithography. Laser interference lithography (LIL) has a strength in this respect [12–14]. LIL is based on the interference of two coherent laser beams incident on a photoresist-coated substrate, as shown in Figure 1(a). The two beams produce a standing wave pattern on the sample surface with a pitch of $d = \lambda/(2\sin\theta)$, where λ is the wavelength of the laser and 2θ is the angle between the two laser beams. Thus, LIL does not need a mask and has a huge advantage for large-area patterning.

This paper reports the fabrication of arrays of magnetic nanowires by using LIL and the magnetic measurements. The length of the wire was much larger than its thickness and width, and the ratio of the width to thickness varied from 8 to 23. We found that this finite ratio

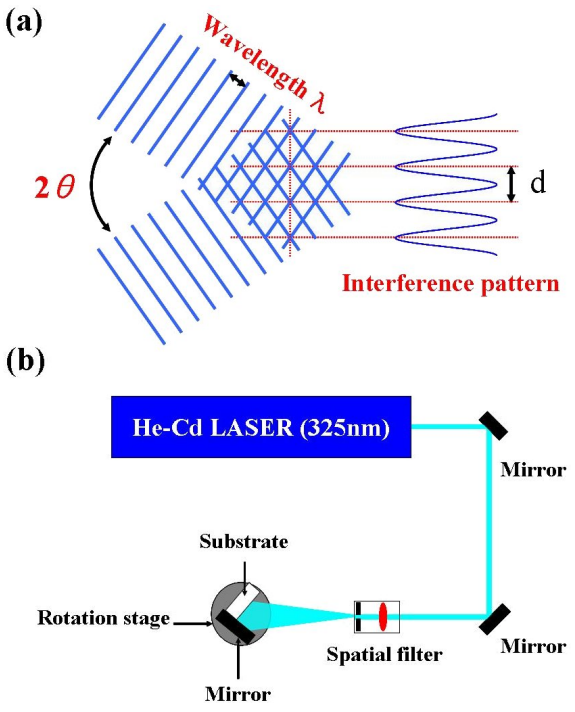

Fig. 1. (a) Basic principle of laser interference lithography (LIL). The distance (pitch) between the intensity maxima is determined by the angle between the two laser beams and the wavelength of the laser. (b) Experimental set-up for laser interference lithography.

*E-mail: jl10017@phya.yonsei.ac.kr; Fax: +82-2-392-1592

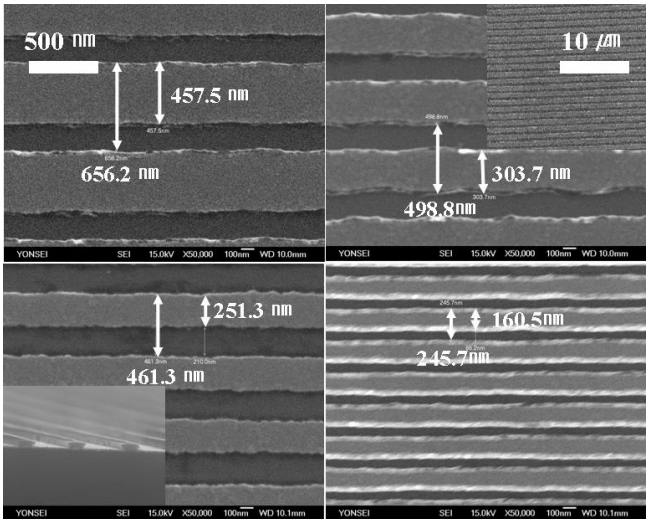

Fig. 2. SEM images of the nanowire arrays. The upper-right inset shows a large-area SEM image and the lower-left inset shows a typical 3-dimensional SEM image of the PR-wire.

directly affected the magnetic hysteresis loops. This result can be well explained by using the simple ellipsoid model.

II. EXPERIMENTS

We have used LIL to produce PR nanowire arrays on a 2 × 2 cm^2 Si substrate. At first, photoresist (MEGA-POSIT SPR 510-A positive)-coated Si substrate was exposed to two expanded HeCd laser beams with a wavelength of $\lambda = 325$ nm. Figure 1(b) shows the experimental configuration for the LIL used by our group. After exposure to the laser beams, the sample is developed to produce an array of PR wires on the Si substrate. A 20 nm thickness of Fe is evaporated on this PR wires/Si in a vacuum chamber with a base pressure 3×10^{-9} Torr. Then, the PR wire is removed by using acetone, which leaves an array of magnetic wires on Si substrate

The exact pitch and width of the wire were determined by using a field emission scanning electron microscope (FESEM: JEOL 6500F). The magnetic hysteresis loops were measured by using the magneto-optic Kerr effect (MOKE) equipment.

III. RESULT AND DISCUSSION

Figure 2 shows SEM images of the wires that were studied in this research, and the insets show a large-area image (upper-right) and a cross-sectional view of a typical PR wire (lower-left). The widths of the wires are 161, 251, 304 and 458 nm, but their lengths are almost

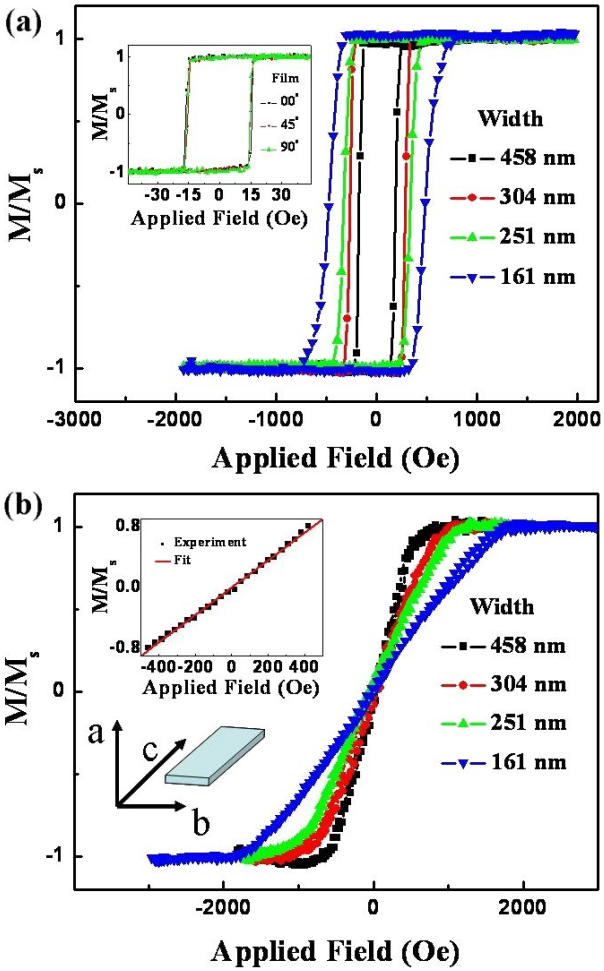

Fig. 3. (a) Magnetic hysteresis loops for nanowire arrays with the applied field along the wire axis. The inset is the hysteresis loops of a 20-nm-thick Fe film with the applied fields in three different directions. (b) Magnetic hysteresis loops for nanowires with the applied field perpendicular to the wire axis in the plane. The inset shows the experimental results in the range of $M/M_S = -0.8 \sim 0.8$ for the wire with a width of 250 nm and the linear fit with Eq. (3).

infinite compared to their widths, as confirmed by the inset. The uniformity of the wire pattern was confirmed by taking SEM images from different parts of the sample. Though the pitch between the wires was determined by the angle between the incident beams, the width of the wire was mainly controlled by the exposure time. The fabrication conditions are summarized in Table 1.

Figure 3(a) shows the magnetic hysteresis loops of the wire arrays for the magnetic fields applied along the wire axis. A 100 % remanent magnetization was observed for all samples, which clearly shows that the wire axis is the easy direction of magnetization. The coercive field decreases with increasing wire width. However, the Fe wire with a 161 nm width shows a relatively smooth switching behavior compared to other wires. The inset shows the magnetic hysteresis loops of the 20-nm-thick Fe film for

Table 1. Summary of the experimental conditions for nanowire fabrication, together with the experimentally determined uniaxial anisotropy constants and the coercive fields. The thickness of the Fe nanowire is 20 nm.

Pitch (nm)	Incident angle	Exposure time (S)	Wire width (nm)	K_u (emu/cm^3)	H_c (Oe)
246	45°	120	161	1.25×10^6	478
461	30°	120	251	8.57×10^5	328
499	20°	120	304	7.14×10^5	277
656	15°	120	458	4.98×10^5	179

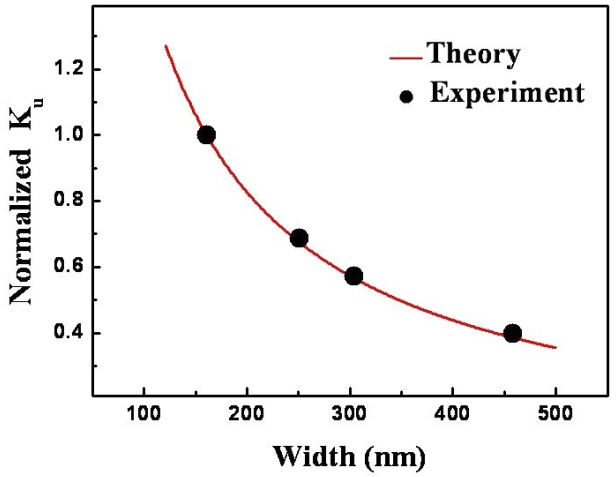

Fig. 4. Variation of the normalized uniaxial anisotropy constant (K_u) vs. wire width. The theoretical values are obtained by using Eq. (2). N_c is neglected in this estimate.

three different applied field directions in the plane. No noticeable difference is observed, which means that the film is magnetically isotropic and has no preferred direction of magnetization. The coercive field (∼16 Oe) is very small compared to the arrays of the patterned wires. These are expected results for non-crystalline magnetic films. Figure 3(b) shows the hysteresis loops when the magnetic field is applied perpendicular to the wire axis in the plane. All wires show hard axis loops with almost zero remanent magnetization. The saturation field increases as the width of the wire decreases. The magnetization varies linearly with the applied field, which is a typical behavior as the magnetization rotates toward the hard axis direction. The uniaxial anisotropy field can be obtained by fitting the linear part of the hard axis loop to a linear function. A ±80 % of magnetization was used for the curve-fit, and the inset shows an example of this fit to the magnetization curve. Table 1 summarizes the results together with the coercive fields for the wire arrays.

The shape-induced magnetic anisotropy can be qualitatively explained by using the simple ellipsoid model, although the shape of the wire is not ellipsoid [9]. When the magnetic field is applied along the hard axis in the plane, the magnetization curve can be expressed as

$$\frac{M}{M_S} = \frac{M_S}{2K_{sh}}H, \tag{1}$$

where K_{sh} is the uniaxial anisotropy constant. If the demagnetizing factors along the three perpendicular axes are expressed as N_a, N_b and N_c as shown in Figure 3(b), then K_{sh} is expressed as $2\pi M_S^2 N_b$. Here, N_c is neglected because the length of the wire is much longer than the width. Figure 3(b) clearly demonstrates that N_b varies as the width of the wire varies. This means that N_a is not negligible. In order to find the effect of N_a on N_b, we used an oblate ellipsoid model. If we put the ratio of the width to the thickness as k, then the demagnetizing factor parallel to the plane of the surface is [15]

$$N_b = \frac{1}{2} = \left\{ \frac{k^2}{(k^2-1)^{(3/2)}} \sin^{-1}\frac{\sqrt{k^2-1}}{k} - \frac{1}{k^2-1} \right\}. \tag{2}$$

Instead of using the calculated K_{sh}, the normalized value, K_u, which can be obtained by dividing all K_{sh} by K_{sh} at 161 nm, can be compared with the experiment because the wire is not an oblate ellipsoid. Figure 4 shows the variation of the normalized uniaxial anisotropy constant, together with experimentally determined ones. Both show the same variation. From this, the observed magnetic anisotropy is solely caused by the shape of the wire.

IV. CONCLUSION

Arrays of magnetic nanowires were fabricated by using the LIL and the liftoff techniques. The observed magnetic anisotropy of the nanowire array and the variation of uniaxial magnetic anisotropy were well explained by using a simple ellipsoid model.

ACKNOWLEDGMENTS

This work was supported by grant No. R01-2004-000-10715-0 from the Basic Research Program of the Korea Science & Engineering Foundation.

REFERENCES

[1] T. A. Moore, A. Ionescu and J. A. C. Bland, J. Appl. Phys. **96**, 6546 (2004).
[2] G. S. S. Beach, C. Nistor, C. Knutson, M. Tsoi and J. L. Erskine, Nature Mater. **4**, 741 (2005).
[3] D. A. Allwood, G. Xiong, M. D. Cooke, C. C. Faulkner, D. Atkinson, N. Vernier and R. P. Cowburn, Science **296**, 2003 (2002).
[4] S. G. Lee, S. W. Shin, J. Lee, J. H. Lee, T. G. Kim and J. H. Song, J. Korean Phys. Soc. **46**, 1170 (2005).

[5] H. M. Hwang, S. W. Shin, J. H. Kang, J. Lee, J. H. Lee, J. H. Song, J.-Y. Choi, H. H. Lee and H. S. Lee, J. Korean Phys. Soc. **49**, 1016 (2006).
[6] T. M. Whitney, J. S. Jiang, P. C. Searson and C. L. Chien, Science **261**, 1316 (1993).
[7] S. J. Blundell, C. Shearwood, M. Gester, M. J. Baird, J. A. C. Bland and H. Ahmed, J. Magn. Magn. Mater. **135**, L17 (1994).
[8] L. Piraux, S. Dubois, E. Ferain, R. Legras, K. Ounadjela, J. M. George, J. L. Maurice and A. Fert, J. Magn. Magn. Mater. **165**, 352 (1997).
[9] L. Sun, P. C. Searson and C. L. Chien, Appl. Phys. Lett. **79**, 4429 (2001).
[10] H. S. Kim, S. Ahn, D. W. Kim, Y. C. Kim and H. W. Kim, J. Korean Phys. Soc. **49**, S712 (2006).
[11] S.-K. Kim, J. Korean Phys. Soc. **50**, 1952 (2007).
[12] J. P. Spallas, R. D. Boyd, J. A. Britten, A. Femandez, A. M. Hawryluk, M. D. Perry and D. R. Kania, J. Vac. Sci. Technol. B **14**, 2005 (1996).
[13] Y. Hao, F. J. Castano, C. A. Ross, B. Vogeli, M. E. Walsh and H. I. Smith, J. Appl. Phys. **91**, 7989 (2002).
[14] J.-S. Kim, K.-D. Lee, S.-W. Ahn, S. H. Kim, J.-D. Park, S.-E. Lee and S.-S. Yoon, J. Korean Phys. Soc. **45**, S890 (2004).
[15] S. Chikazumi, *Physics of Ferromagnetism*, 2nd ed. (Clarendon Press, Oxford, 1997), p. 14.